IS THE X-RAY SPECTRUM OF THE SEYFERT 2 GALAXY NGC 5252 INTRINSICALLY FLAT?

M. CAPPI,[1] T. MIHARA,[1] M. MATSUOKA,[1] W. BRINKMANN,[2] M. A. PRIETO,[2] AND G. G. C. PALUMBO[3,4]

ABSTRACT

The first X-ray observation of the Seyfert 2 galaxy NGC 5252 is reported. *ASCA Astro-D* collected approximately 4000 photons per detector, enough to perform an accurate spectral analysis of this source. The luminosity of NGC 5252 is $L_X(0.7–10 \text{ keV}) \simeq 2.6 \times 10^{43}$ ergs s^{-1}, typical of a Seyfert 1 galaxy. A simple description of the spectrum with a single power law is ruled out by the SIS data, which shows a strong soft excess at $E \lesssim 1.2$ keV. The spectrum is best fitted by models assuming either partial covering of the central source or scattering of the X-ray continuum. The best-fit partial covering model results in a flat ($\Gamma \simeq 1.45 \pm 0.2$) power-law continuum emitted by a source almost completely covered (at $\sim$94%–97%) by neutral matter [$N_H \simeq (4.3 \pm 0.6) \times 10^{22}$ cm^{-2}]. The detected iron line is remarkably weaker (EW $\simeq 90 \pm 60$ eV) than normally found from Seyfert 2 galaxies. In an effort to interpret the observed flat spectrum with an intrinsically steep power law as predicted by unified models, we also included in the models neutral reflection, ionized absorption (warm absorber), and nonuniform cold absorption (dual-absorber). We find that the observed flat continuum *and* weakness of the iron line pose a problem for neutral reflection models, whatever the assumed geometry is. The use of an ionized absorber (scattering + warm-absorber model) instead of a neutral absorber seems unjustified with the present data. The "dual-absorber" model, representing nonuniform (density) absorption along the line of sight, may provide an alternative explanation for the flatness of the spectrum, with no constraints on the Fe K emission line. Another plausible interpretation of the present data is that the X-ray spectrum of NGC 5252 is truly intrinsically flat. Its strong similarities with the well-known Seyfert 1.5 galaxy NGC 4151 are briefly discussed.

Subject headings: galaxies: individual (NGC 5252) — galaxies: Seyfert — X-rays: galaxies

1. INTRODUCTION

The discovery of broad emission lines in the polarized optical spectra of several Seyfert 2 galaxies (Antonucci & Miller 1985; Miller & Goodrich 1990; Tran, Miller, & Kay 1992) has provided the basis for a unified model of Seyfert galaxies in which the main discriminating parameter between Seyfert 1 and Seyfert 2 nuclei is the inclination to our line of sight of an obscuring torus surrounding the central source (see Antonucci 1993 for a review). In this scheme, Seyfert 1 galaxies are active nuclei observed nearly perpendicularly to the torus plane (unabsorbed), whereas Seyfert 2 galaxies represent those seen through the torus (absorbed). Further support of this scenario has come from *GINGA* X-ray observations, which revealed the strongly absorbed spectra of some Seyfert 2 galaxies (Koyama et al. 1989; Awaki et al. 1991).

NGC 5252 is an S0 galaxy at a redshift of $z \simeq 0.0234$. Its optical size is $\sim 1.4 \times 0.9$, with the major axis being at a position angle P.A. $\sim 15°$, and the absolute visual magnitude is $M_v = -21.4$ (Unger et al. 1987). NGC 5252 harbors a Seyfert 2 nucleus that illuminates a perfectly defined biconical structure of ionized gas extending up to 35 kpc from the nucleus (Tadhunter & Tsvetanov 1989). This is one of the largest extended ionized gas regions among nearby active galactic nuclei (AGNs). The axis of the bi-cone lies roughly at P.A. $\simeq 166°$, close to the main axis of the 20 cm radio structure

($\simeq 172°$). VLA H I observations of this galaxy revealed the existence of neutral gas located just outside the bicone of ionized gas. These findings provided unambiguous proof of the anisotropy of the radiation field in this galaxy (Prieto & Freudling 1993). Additional radio observations have detected weak, narrow extended features aligned with the larger scale optical ionization cones, which further supports the existence of collimation effects in NGC 5252 (Wilson & Tsvetanov 1994).

Because of its favorable orientation with respect to the observer, NGC 5252 is an ideal target for studying the collimation mechanism responsible for the observed anisotropy. Combined near-IR and optical imaging have revealed the presence of a band of material across the nucleus and perpendicular to the bi-cone of ionized gas (Kotilanien & Prieto 1994). The band shows a gradually increasing extinction toward the center of the galaxy; a lower limit to the extinction of 6 mag is estimated.

Near-IR spectroscopy of He I 1.083 μm by Ruiz, Rieke, & Schmidt (1994) shows indeed a broad He I component with FWHM ~ 1050 km s^{-1}, thus revealing the typical signature of a Seyfert 1 nucleus. Polarization studies aimed at discovering the nature of the obscured nucleus via the nuclear light scattered by the surrounding material are not yet conclusive. Optical spectropolarimetry of the galactic nucleus indicates an (11 ± 11)% polarization (Kay 1994). Given the strong (larger than 90%) stellar contribution to the nuclear optical light in this Seyfert 2 galaxy, polarization dilution by stellar light could be significant (Kay 1994; Kotilanien & Prieto 1994); alternatively, scattered light could also suffer extinction.

At the opposite extreme of the electromagnetic spectrum, broadband X-ray data can provide crucial information on the hidden source because photons of a few keV may pass through the nuclear intervening material. It should be noted that since

[1] The Institute of Physical and Chemical Research (RIKEN), 2-1, Hirosawa, Wako, Saitama 351-01, Japan.
[2] Max-Planck-Institut für extraterrestrische Physik, D-85748 Garching bei München, FRG.
[3] Dipartimento di Astronomia, Università di Bologna, Via Zamboni 33, I-40126 Bologna, Italy.
[4] Istituto per le Tecnologie e Studio Radiotervestri, CNR (ITeSRE), CNR, Via Gobetti 101, I-40129, Bologna, Italy.

141

TABLE 1

SELECTION CRITERIA

GIS	SIS
SAA = 0	SAA = 0
COR_MIN > 7	COR_MIN > 6
ELV_MIN > 5°	ELV_MIN > 5°
...	BR_EARTH > 25°
...	T_DY_NT > 100 s

NOTES.—SAA, South Atlantic Anomaly; COR_MIN, cut-off rigidity (GeV/c); ELV_MIN, Minimum elevation angle from earth; BR_EARTH, Minimum bright earth angle; T_DY_NT, Time after a day/night transition.

NGC 5252 is an early-type galaxy, the contribution from star formation activity to the X-ray emission is expected to be minor. Indeed, deep Hα imaging (Prieto & Freudling 1995) shows no trace of ionized gas outside the $[O\ III]_{5007Å}$ ionized bi-cone reported by Tadhunter & Tsvetanov (1989); most of this gas extends out of the galaxy plane. NGC 5252 was not detected in the *ROSAT* all-sky survey. Based on these general considerations, we investigated the X-ray properties of NGC 5252 with the *Advanced Satellite for Cosmology and Astrophysics (ASCA)* observatory. To our knowledge, there is no report of any X-ray detection from previous missions. During the *ASCA* observations, enough photons were collected (§ 2) to allow a detailed and accurate spectral analysis (§ 3). This analysis is discussed in the light of recent observations of Seyfert galaxies and the theoretical models (§ 4). Our main results are summarized in § 5.

2. *ASCA* DATA REDUCTION

ASCA observed NGC 5252 between 1994 January 28 and January 31 with the Gas Imaging Spectrometer (GIS) for a total effective exposure time of about 70,500 s, and with the Solid-State Imaging Spectrometer (SIS) for about 65,000 s. The SIS was operating in 1 or 2 CCD mode and all the data were collected in FAINT mode. Dark frame error (DFE) and echo corrections have been applied to the data (Otani & Dotani 1994). Good observational intervals were selected by applying the data selection criteria shown in Table 1.

Source counts were collected from a circle centered on the source of 4′ radius for the GIS and 2.5 for the SIS. Background spectra were obtained using similar areas inside the field of view (FOV) from uncontaminated regions. We checked for differences between different extraction regions for the source and the background but did not find any significant variations in the spectral results. In the GIS FOV, we detected elongated spurious emission in the direction northwest of NGC 5252. This emission occurs in the direction of the ionized cones, but we can exclude the possibility that it is related to NGC 5252 because of the high separation (~10′) between the two. It is

more likely associated with the bright SB galaxy MCG −01-35-024 whose position is coincident with the emitting region to within ~2′. We emphasize that the use of blank sky backgrounds for the GIS and SIS yielded spectral results within the errors reported in the following spectral analysis.

Relevant data for the NGC 5252 observation are summarized in Table 2. Data preparation and analysis have been done using version 1.0h of the XSELECT package; spectral analysis has been performed using version 8.5 of the XSPEC program (Arnaud et al. 1991).

3. SPECTRAL ANALYSIS

Source plus background light curves were computed in different energy bands: in the broad (0.4–10 keV), the soft (0.4–2 keV), and the hard (2–10 keV) energy bands. None of these light curves indicated significant variability; statistical χ^2 tests against constancy give a probability greater than 15% in every case, i.e., consistent with constant source flux.

Therefore, we accumulated spectra from the photons collected in the total ~70 ks observation for the spectral analysis. The pulse height spectra were binned in such a way that there were at least 30 and 20 counts per bin for the GIS and SIS detectors, and the corresponding energy bands were limited to 0.7–10 keV and 0.4–10 keV, respectively. We used the detector response matrices gisv3_1.rmf (GIS, released in 1994 March) and rsp1.1.alpha (SIS, released in 1994 June) and constructed the effective area at the source position with the program jbldarf-0.5a (released in 1994 January).

3.1. *Single Power-Law Fits*

A single absorbed power-law model was first fitted to the data with the effective hydrogen column density (N_H) left free to vary. The resulting best-fit parameters are given in Table 3. This simple model yielded an acceptable description of the GIS data in the 0.7–10 keV band, with $\chi^2_{red}/dof \simeq 1.03/267$, but gives an unacceptable fit to the SIS data in the 0.4–10 keV band, with $\chi^2_{red}/dof \simeq 1.38/315$. The corresponding SIS spectrum is shown in Figure 1. The residuals of the SIS spectrum clearly indicate the presence of strong soft ($E \lesssim 1.2$ keV) X-ray emission in excess to the extrapolation of the higher energy continuum. It should be pointed out that the discrepancies between the GIS and SIS results (Table 3) are strongly reduced when the soft excess is explicitly fitted in the SIS spectrum, as shown in the following sections. In all fits, the best-fit value of N_H is at least two orders of magnitude higher than the Galactic absorption $N_{Hgal} \simeq 1.97 \times 10^{20}$ cm^{-2} (Dickey & Lockman 1990), suggesting strong intrinsic absorption.

It should be emphasized that, for completeness, an absorption component with $N_H = N_{Hgal}$ was also added to each model tested below in order to account for the absorption in our own galaxy. Because of its low value, however, the Galactic column is effective only at energies $E \lesssim 0.4$ keV.

TABLE 2

EXPOSURE TIMES AND COUNT RATES

Detector	Exposure (s)	Source + Background (counts)	Background (counts s^{-1})	Source (counts s^{-1})
GIS2......	70,970	4011	0.011	0.045
GIS3......	70,747	5194	0.012	0.061
SIS0	65,154	4235	0.010	0.055
SIS1	64,448	3736	0.008	0.050

TABLE 3
GIS AND SIS: SINGLE POWER LAW

Detector	N_H $(10^{22}$ cm$^{-2})$	Γ	F_X^a(0.7–10 keV) $(10^{-12}$ ergs cm^{-2} s$^{-1})$	χ^2_{red}/dof
GIS2......	$3.76^{+0.84}_{-0.75}$	$1.35^{+0.25}_{-0.24}$	8.23	0.83/118
GIS3......	$3.91^{+0.71}_{-0.63}$	$1.43^{+0.20}_{-0.20}$	9.77	0.99/146
Both	$3.83^{+0.54}_{-0.49}$	$1.39^{+0.16}_{-0.15}$	9.00	1.03/267
SIS0	$2.13^{+0.73}_{-0.52}$	$0.84^{+0.31}_{-0.24}$	9.00	1.39/165
SIS1	$2.52^{+0.73}_{-0.52}$	$1.05^{+0.32}_{-0.30}$	9.46	1.36/145
Both	$2.34^{+0.48}_{-0.44}$	$0.95^{+0.20}_{-0.20}$	9.20	1.38/313

NOTE.—Intervals are at 90% confidence for two interesting parameters.
[a] Corrected for absorption.

3.2. Soft Excess

3.2.1. Thermal Soft-Emission Models

In a first attempt to model the soft X-ray excess, the broadband pulse-height spectrum was fitted with the following two-component models: (a) black body + absorption × power law, (b) bremsstrahlung + absorption × power law and (c) Raymond Smith + absorption × power law, with the absorption applied to the power law free to vary in all models.

In model a, the blackbody emission component could mimic the high energy tail of the spectrum emitted by an accretion disk. In models b and c, it is assumed that the soft X-ray emission is produced by a thermal thin and hot gas associated with the host galaxy. In all three models, the hard power law is thought to be related to the nucleus itself. With all parameters free to vary, these models yielded acceptable fits to the SIS data

with χ^2_{red}/dof ~ 0.93–1.1/311. Our results are reported in Table 4. All these models yielded similar values of N_H.

Fitting with model a gave L_X(0.1–2.0 keV) $\simeq$ 3.9 × 10^{41} ergs s^{-1} and a blackbody temperature of $T \simeq 2 \times 10^6$ K. From these values, we deduce a characteristic dimension of the emitting region of $r \simeq 3 \times 10^9$ cm, which is two orders of magnitude smaller than the Schwarzschild radius for a 10^6 $M_\odot$ black hole. Therefore, a blackbody + power law model does not provide a physically meaningful description of the data.

Thermal bremsstrahlung (model b) with a characteristic temperature of approximately 0.8 keV, together with a hard power law with $\Gamma \simeq 1.3 \pm 0.2$, provides a possible description of the data. However, this interpretation is inconsistent with the lack of soft emission lines in the ASCA spectrum, which are expected to be emitted by a hot ($T \sim 10^7$ K) plasma. The same problem is faced by a Raymond-Smith model (model c;
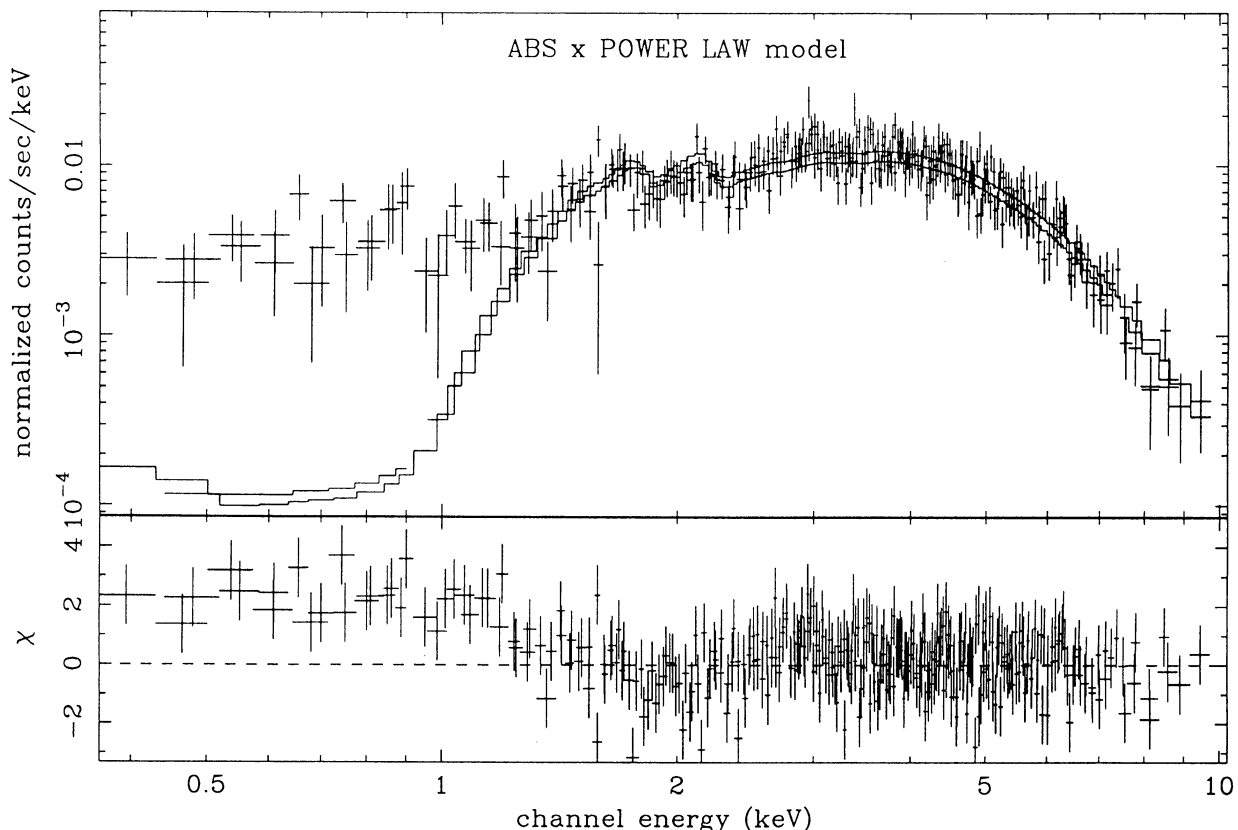

FIG. 1.—SIS spectrum and associated residuals obtained from the simultaneous joint fit of SIS0 and SIS1 instrument data with a single absorbed power law. The solid line represents the best-fit power law modeled to the spectrum between 0.4–10 keV. A soft excess below 1.2 keV is clearly evident.

TABLE 4
SIS: TWO-COMPONENT MODELS

Model	Abundance	kT (keV)	N_H $(10^{22}$ cm$^{-2})$	Γ	L_X[a] (0.1–2.0 keV) $(10^{41}$ ergs s$^{-1})$	χ^2_{red}/dof
Blackbody + absorption (PL)	...	$0.18^{+0.05}_{-0.03}$	$3.04^{+0.74}_{-0.53}$	$1.17^{+0.20}_{-0.16}$	3.86	0.94/311
Bremsstrahlung + absorption (PL)......	...	$0.80^{+1.23}_{-0.33}$	$3.45^{+0.83}_{-0.62}$	$1.26^{+0.26}_{-0.24}$	6.47	0.93/311
R-S[b] + absorption (PL)	<0.01	$0.77^{+1.18}_{-0.24}$	$3.46^{+0.84}_{-0.66}$	$1.26^{+0.23}_{-0.18}$	6.44	0.92/310

NOTE.—Intervals are at 90% confidence for three interesting parameters.
[a] Calculated with only the soft component.
[b] R-S denotes Raymond-Smith.

Raymond & Smith 1977). In this case, metal abundances below approximately 0.01 solar are needed for acceptable fits, as reported in Table 4. These results, together with general arguments concerning the host galaxy (see § 4.1), make the hypothesis of a thermal origin for the soft excess unlikely in the case of NGC 5252.

3.2.2. Partial Covering Model

The observed SIS spectrum was then fitted with a partial covering model (Holt et al. 1980). This model consists of a power-law continuum obscured by cold uniform matter with column density N_H, which covers fraction C_F of the source. The model has four free parameters, namely the normalization, the photon index, the covering fraction, and the column density. In physical terms, the absorbing material might be identified with thick and cold clouds distributed along the line of sight, covering only part of the central source.

As illustrated by the unfolded spectrum in Figure 2, this model provides a good description of the SIS (0.4–10 keV) spectrum, with χ^2_{red}/dof $\simeq 0.95/315$. The best-fit parameters are reported in Table 5a. Confidence contours for the photon index versus column density and for the covering fraction versus column density are shown in Figure 3. The best-fit parameters show that the SIS spectrum of NGC 5252 is consistent with a flat ($\Gamma \simeq 1.45 \pm 0.2$) underlying power law viewed through an absorber with column density $N_H \simeq (4.3 \pm 0.6) \times 10^{22}$ cm^{-2} that covers approximately 96% of the primary source. The absorption-corrected flux between 0.4–10 keV is 11.7×10^{-12} ergs cm^{-2} s^{-1}. We emphasize that the reported errors correspond to 90% confidence limits for three inter-
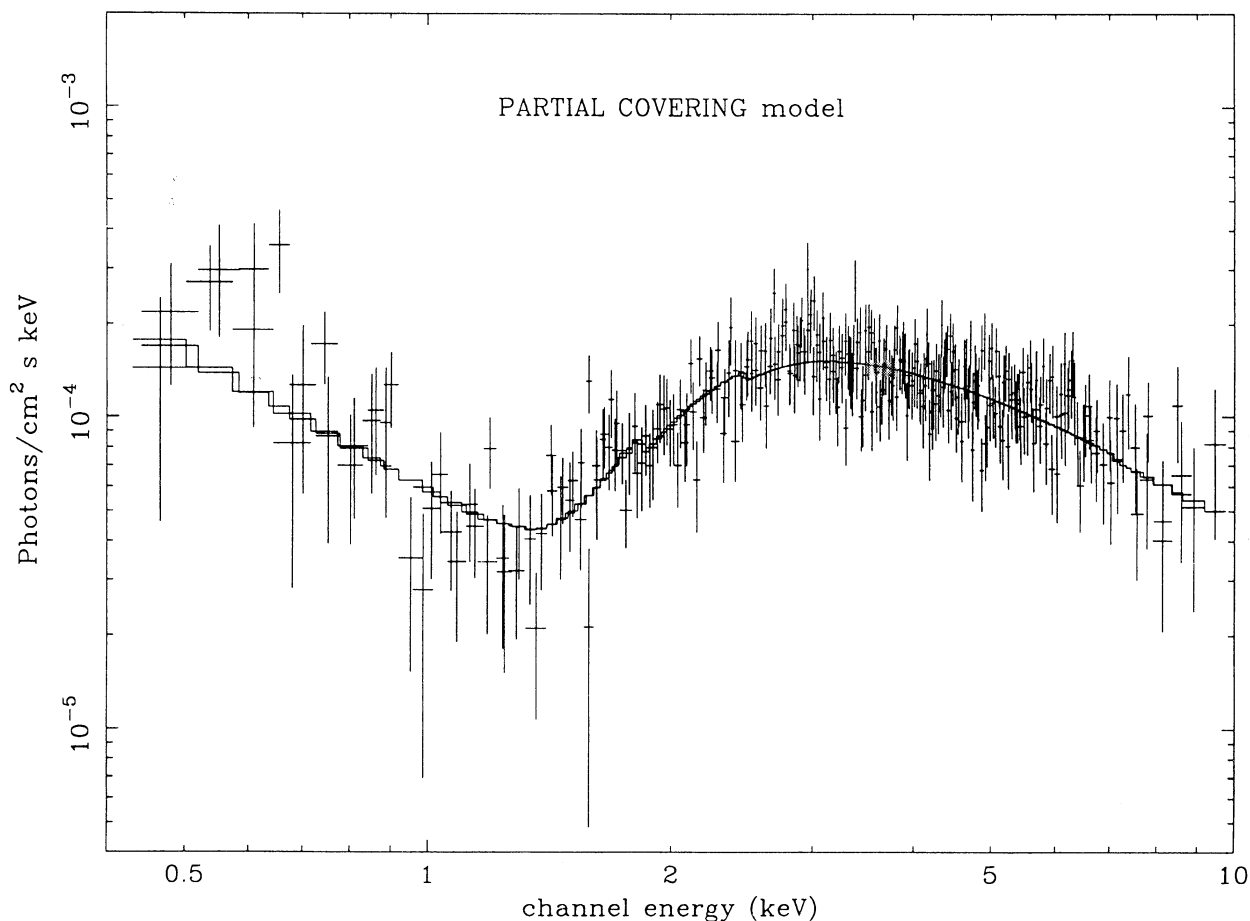

FIG. 2.—Unfolded SIS spectrum with the partial covering model. The solid line represents the best-fit partial covering model.

TABLE 5A

SIS: PARTIAL COVERING MODEL

N_H $(10^{22} \text{ cm}^{-2})$	C_F	Γ	F_χ^a (0.4–10 keV) $(10^{-12} \text{ ergs cm}^{-2} \text{ s}^{-1})$	χ^2_{red}/dof
$4.33^{+0.66}_{-0.61}$	$0.96^{+0.01}_{-0.02}$	$1.45^{+0.23}_{-0.23}$	11.69	0.95/312

TABLE 5B

SIS: SCATTERING MODEL

N_H $(10^{22} \text{ cm}^{-2})$	$A(1)/A(2)^b$	Γ	F_χ^a (0.4–10 keV) $(10^{-12} \text{ ergs cm}^{-2} \text{ s}^{-1})$	χ^2_{red}/dof
$4.39^{+0.68}_{-0.64}$	0.046	$1.46^{+0.23}_{-0.23}$	11.69	0.95/312

NOTE.—Intervals are at 90% confidence for three interesting parameters.

^{a} Corrected for absorption.

^{b} $A(1)/A(2)$ = (normalization of the scattered component at 1 keV)/(normalization of the continuum at 1 keV).

esting parameters and are therefore very conservative limits (Lampton, Margon, & Bowyer 1976).

The derived N_H value is equivalent to $A_V \sim 20$ mag, for a standard gas to dust ratio, and thus is consistent with the large extinction toward the central source predicted from the IR-optical data (Kotilanen & Prieto 1994).
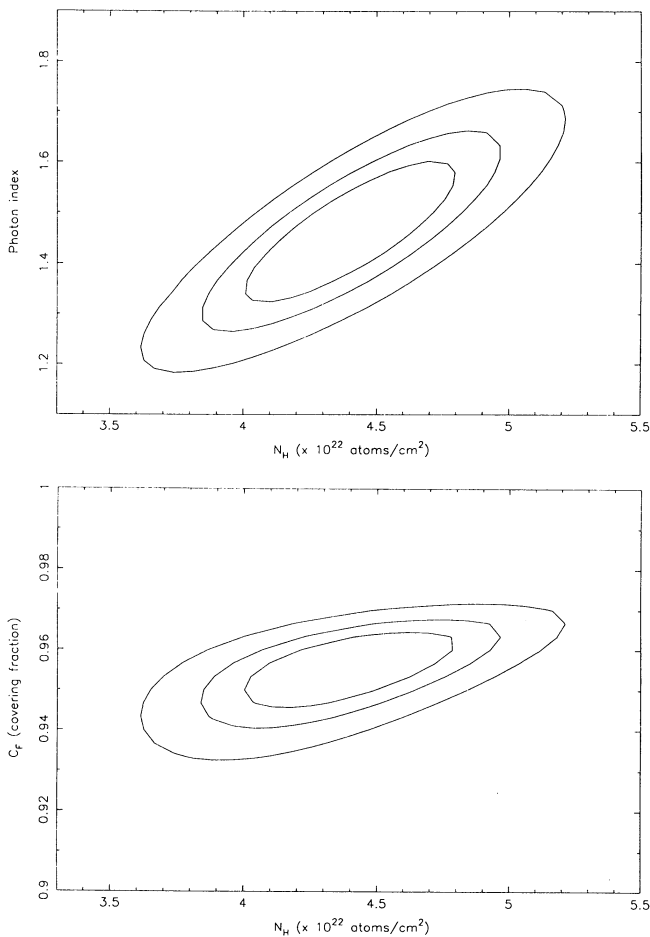

FIG. 3.—Confidence contours for photon index vs. column density (top) and covering fraction vs. column density (bottom) for the best fit obtained with the partial covering model. Contours are at 68%, 90%, and 99% confidence levels.

It should be pointed out that with the partial covering model, the shape of the power law in the SIS is consistent with the results obtained from the GIS instrument with a single power-law model (§ 3.1). Fitting the GIS data with a partial covering model, one obtains best-fit parameters which agree with the SIS results within approximately 3%.

3.2.3. Scattering Model

Another model which could describe the soft excess is a scattering model. Numerically equivalent to the partial covering model, it consists of the sum of two power laws having the same photon index but different absorptions and normalizations. One power law is absorbed by the Galactic column density only and the other is absorbed by a high intrinsic column density (a free parameter during the fit procedure). In this model the "non-absorbed" and absorbed power laws are related to the presence of scattering and obscuring matter, respectively. This interpretation is supported by unified models of AGNs, which predict that the direct continuum of Seyfert 2 galaxies is strongly obscured by a thick torus (Ghisellini, Haardt, & Matt 1994), whereas part of the nuclear emission is scattered by free electrons surrounding the broad-line region (BLR) (Antonucci & Miller 1985; Awaki et al. 1991).

As reported in Table 5b, the scattering model yields a good description of the data with $\chi^2_{red}/\text{dof} \simeq 0.95/312$, the best-fit parameters being again a flat power law with $\Gamma \simeq 1.46 \pm 0.2$, intrinsic absorption $N_H \simeq (4.4 \pm 0.6) \times 10^{22}$ cm^{-2} ($\sim N_H$ partial covering), and a fraction of $\simeq 4\%$–5% of the continuum scattered into the observer's line of sight.

3.3. Flat Spectrum

On one side, HEAO 1 A-2 (Weaver, Arnaud, & Mushotsky 1995) and Ginga (Nandra & Pounds 1994) results have shown that the observed canonical photon index $\Gamma_{2-18\text{keV}} \sim 1.7$–1.8 of Seyfert 1 galaxies can be interpreted as the sum of a steep intrinsic power law with $\Gamma_{2-18\text{keV}} \sim 1.8$–2.1 and a reflection component (e.g., Lightman & White 1988). On the other side, we still do not know very much about Seyfert 2 galaxies, as they are generally more absorbed, and only few of them have high signal-to-noise ratio (S/N) X-ray spectra. Seyfert unification models (e.g., Antonucci 1993) predict the same average intrinsic photon index for Seyfert 1 and Seyfert 2 galaxies, but there is increasing evidence that the observed photon indices of several Seyfert 2 galaxies are flat with $\Gamma_{2-10\text{keV}} \sim 1.4 \pm 0.2$ (Awaki et al. 1991; Kunieda et al. 1994). Whether the intrinsic

photon index of these is flat or not is an important question that directly impacts Seyfert unification models.

We have shown that all the models applied to NGC 5252 require a flat power law. In light of the above considerations, it is therefore tempting to use more complex models to search for a global description of the spectrum with an intrinsically steep power law, as predicted by unified models. Therefore, in the following sections, we will focus on models involving (a) reflection by thick material, (b) absorption by ionized matter, and (c) line of sight obscuration. These models will be used together with the partial covering model (a and c) or scattering model (b). It should be borne in mind that though they imply different physical interpretations, the partial covering and scattering models cannot be distinguished with the present data (§ 4.1) and would therefore give equivalent results if interchanged.

3.3.1. Reflection Component and Composite Models

We first considered the possibility of explaining the apparently flat spectrum of NGC 5252 with the presence of a reflection component. The existence of cold gas responsible for radiation reprocessing near the center of AGN is suggested by the strong UV emission in many observed AGN and is supported by theoretical considerations (Guilbert & Rees 1988). It is well established that the presence of this reflecting matter can strongly modify the observed X-ray spectrum. In particular, it could flatten the observed continuum (Lightman & White 1988) and provide an excellent explanation for at least part, if not all, of the iron emission line intensity.

The reflection model used in the present analysis is the general case of neutral reflection from a slab of optically thick matter with $\tau_T \gg 1$ proposed by Lightman & White (1988), with opacities taken from Morrison & McCammon (1983). The spectrum is calculated integrating over all viewing angles and assuming isotropic emission from the source. The model used is the "plrefl" reflection model available in the XSPEC fitting package (Arnaud et al. 1991). This model requires a total of five parameters, namely, the photon index (Γ_{int}) and normalization (A_{pl}) of the primary power law, the normalization of the reflected component (A_{refl}), the slab inclination (i), and the fraction of the solid angle subtended by the slab ($\Omega/2\pi$). The latter parameter ($\Omega/2\pi$) has been fixed to 1 because it is redundant with A_{refl} in the fitting procedure. The inclination i was fixed to 0 (slab assumed face-on) because the shape of the reflected continuum is only a weak function of the inclination. In its simplest form, the one used here, this model is completely determined by only three (free) parameters (Γ_{int}, A_{pl}, and A_{refl}). By examining the ratio $R \equiv A_{refl}/A_{pl}$, we can then make inferences about these parameters. For example, a value of $R \sim 1$ is consistent with an isotropic source covered by $\Omega/2\pi \sim 1$. A value of $R > 2$ cannot be explained with only an increase in $\Omega/2\pi$ but requires a time lag effect or/and anisotropic emission from the source.

This model was combined together with the partial covering model (§ 3.2.2), yielding a total of five free parameters (one additional one if compared to the single partial covering model). The photon index was left free to vary. The resulting best-fit parameters are reported in Table 6, and the best-fit model is shown in Figure 4. The inclusion of a reflection component improves the fit by $\Delta\chi^2 \sim 6$, which is significant at more than 95% significance level for the addition of one free parameter. The resulting amount of reflection is $R \simeq 7.2^{+7.6}_{-5}$, and the photon index is $\Gamma \simeq 1.91 \pm 0.33$. The errors quoted here and below in this work represent 90% confidence intervals

TABLE 6
SIS: Partial Covering + Reflection

N_H $(10^{22} \text{ cm}^{-2})$	C_F	A_{pl} [a]	A_{refl} [a]	Γ_{int}	χ^2_{red}/dof
$4.61^{+0.40}_{-0.39}$	$0.97^{+0.01}_{-0.01}$	2.19	$15.6^{+16.3}_{-12.3}$	$1.91^{+0.33}_{-0.33}$	0.92/311

Note.—Intervals are at 90% confidence for one interesting parameter.
[a] Normalization at 1 keV in units of 10^{-3} photons cm^{-2} s^{-1} keV^{-1}

for one interesting parameter ($\Delta\chi^2 = 2.701$; Avni 1976). It is clear from these values and from Figure 4 that a very strong reflection component is necessary if one wants to model the observed flat shape at energies $4 < E < 10$ keV with an underlying steep power law.

The data are therefore consistent with an intrinsically steep ($\Gamma \sim 1.9$) power law, provided that there is a very strong ($R \sim 7$) reflection component. However, as will be discussed later (§ 4.2), the presence of such a strong reflection is unlikely, though not ruled out, in NGC 5252 because it predicts a stronger than observed iron Kα line (§ 3.4).

3.3.2. Warm Absorber and Composite Models

We further investigated the possibility that a steep ($\Gamma = 1.9$) power law passing through a warm absorber can give an apparently flat 0.4–10 keV spectrum. In contrast to a neutral absorber (where we use a partial covering model), this model interprets absorption as being due to highly ionized gas that completely covers the continuum source. The presence of absorption due to ionized matter has currently been confirmed in several Seyfert 1 galaxies (see Matsuoka 1994 for a review) and may also contribute significantly to the soft X-ray emission of intermediate Seyfert galaxies such as NGC 4151 (Weaver et al. 1994b). We therefore investigated whether a warm absorber can explain both the soft excess and flat spectrum of NGC 5252.
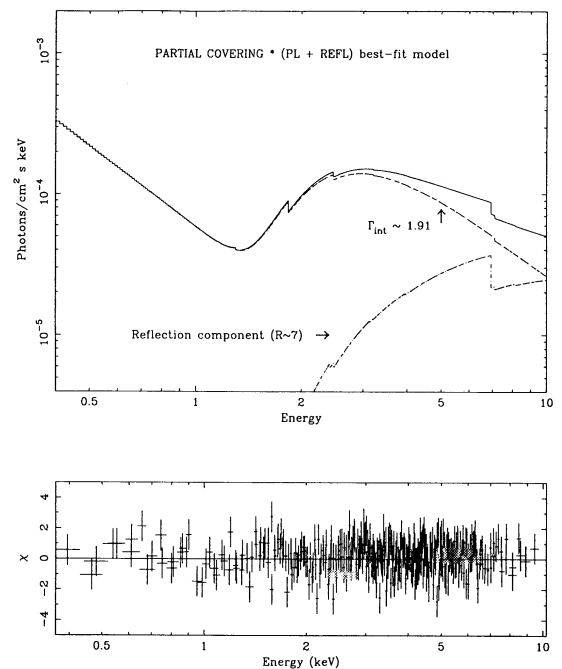

Fig. 4.—SIS best-fit model and associated residuals with the partial covering + reflection component model.

A simple model of a warm absorber using the "CLOUDY" photoionization code (Ferland 1991) has been constructed. Following Fabian et al. (1994), we assumed that a shell of gas with solar abundances, density 10^8–10^{10} cm^{-3}, and uniform temperature is uniformly distributed around an ionizing power law continuum source with $\Gamma = 1.9$ and luminosity $L = 10^{43}$ ergs s^{-1}. The emergent spectrum, consisting of the transmitted continuum plus the emission from the shell, was fitted to the SIS data. The free parameters were the "warm" column density N_W (cm^{-2}), the ionization parameters $\xi = L/nR^2$ (ergs s^{-1} cm), and the normalization constant of the warm absorber model. The model gave a poor fit to the data (with $\chi^2_{red}/$dof = 1.32/314, and strong systematic differences between the model and the data were evident between 0.7 and 1.6 keV. Indeed, the warm absorber hypothesis does not work unless another soft component is added because the strong edges around 1 keV predicted by the model (Netzer 1993; Krolik & Kriss 1995) are not seen in the data.

We then repeated the fitting procedure with an additional power law to mode a soft scattered component (increasing the number of free parameters to five). The photon index of the warm absorbed power law was again fixed to 1.9, but that of the scattered component was free to vary. All other parameters were also varying. The resulting composite scattering + warm absorber model yielded an acceptable fit, with $\chi^2_{red}/$dof $\simeq$ 0.96/311. The best-fit model is shown in Figure 5, and the interesting best-fit parameters are $\log N_W \simeq 22.88 \pm 0.02$, $\log \xi \simeq 1.61 \pm 0.04$, and $\Gamma \simeq 1.43^{+0.41}_{-0.73}$ for the scattered component. For two interesting parameters, the 90% upper limit for the photon index of the scattered component is approximately 1.92.

Thus, when the spectrum of NGC 5252 is modeled with a composite warm absorber plus (scattered) power law, an intrinsic index as steep as 1.92 cannot be ruled out. However, despite the higher number of free parameters, the statistics are worse than with the single partial covering model, probably because of the presence of systematic positive residuals at high ($E > 6$ keV) energies (Fig. 5).

3.3.3. Composite "Dual-Absorber" Model

A further possibility to mask a steep intrinsic continuum slope is through the presence of an additional, strongly absorbed power law. This could considerably flatten the observed spectrum in the *ASCA* energy band, similar to a very strong reflection component. We then fitted the data by adding a second absorbed power law to the partial covering model. The resulting spectral model can be interpreted as a single power law undergoing absorption by material with two different column densities that partly, but not completely, cover the source. For example, this may be a crude approximation of a nonuniform density distribution of clouds along the line of sight.

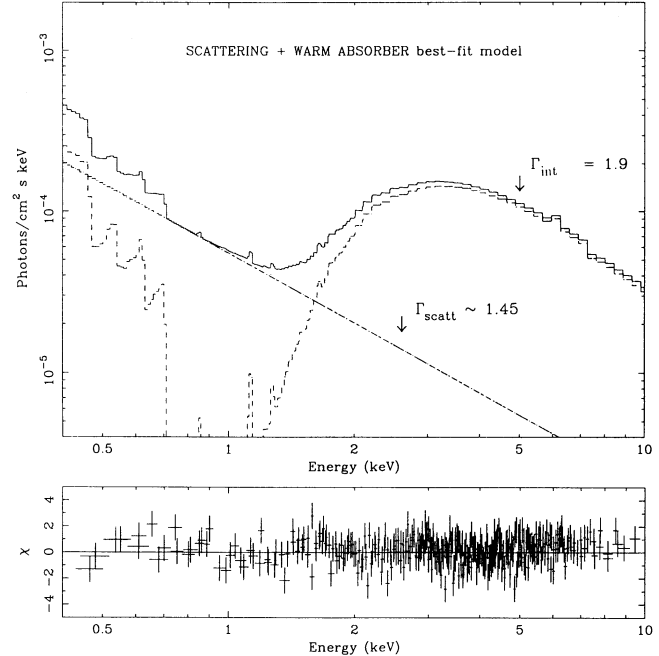The resulting composite "dual-absorber" model is of the

FIG. 5.—SIS best-fit model and associated residuals with the scattering + warm absorber model.

following form: partial covering absorption × power law (1) + partial covering absorption × power law (2). Photon indices and covering fractions were fixed to be equal for both components, leading to a total of six free parameters, namely, the two different absorptions (N_{H1} and N_{H2}), the two normalizations $A(1)$ and $A(2)$, the covering fraction C_F, and the photon index.

The model yielded an acceptable description of the source spectrum with $\chi^2_{red}/$dof $\simeq$ 0.92/311. The resulting best-fit parameters reported in Table 7 are consistent with an intrinsically steep ($\simeq 1.86 \pm 0.3$) power law source almost completely ($\sim 98\%$) covered by two distinct absorption columns with approximately 4.8×10^{22} cm^{-2} (for $\sim 55\%$ of the covering matter) and approximately 6.2×10^{23} cm^{-2} (for $\sim 45\%$ of the covering matter). As is evident from the best-fit model shown in Figure 6a, the strongly absorbed power law could well flatten the hard part of the spectrum in the *ASCA* energy band. Therefore, this model provides a viable description of the spectrum of NGC 5252 consistent with a steep power law. It will be considered again in § 4.2.

The results obtained wih the scattering model are also shown for comparison in Figure 6b. As stated above, the fits are algebraically equivalent, but in the scattering case the spectral model could be related to a physical scenario in which the continuum is (completely) covered by a torus of nonuniform

TABLE 7

SIS: COMPOSITE DUAL-ABSORBER MODEL

N_{H1} (10^{22} cm^{-2})	$A^a(1)$	C_F	Γ	N_{H2} (10^{22} cm^{-2})	$A^a(2)$	$\chi^2_{red}/$dof
$4.82^{+0.40}_{-0.37}$	2.17	$0.98^{+0.01}_{-0.01}$	$1.86^{+0.26}_{-0.31}$	62^{+64}_{-25}	1.75	0.92/311

NOTE.—Intervals are at 90% confidence for one interesting parameter.
[a] Normalization at 1 keV in units of 10^{-3} photons cm^{-2} s^{-1} keV^{-1}.
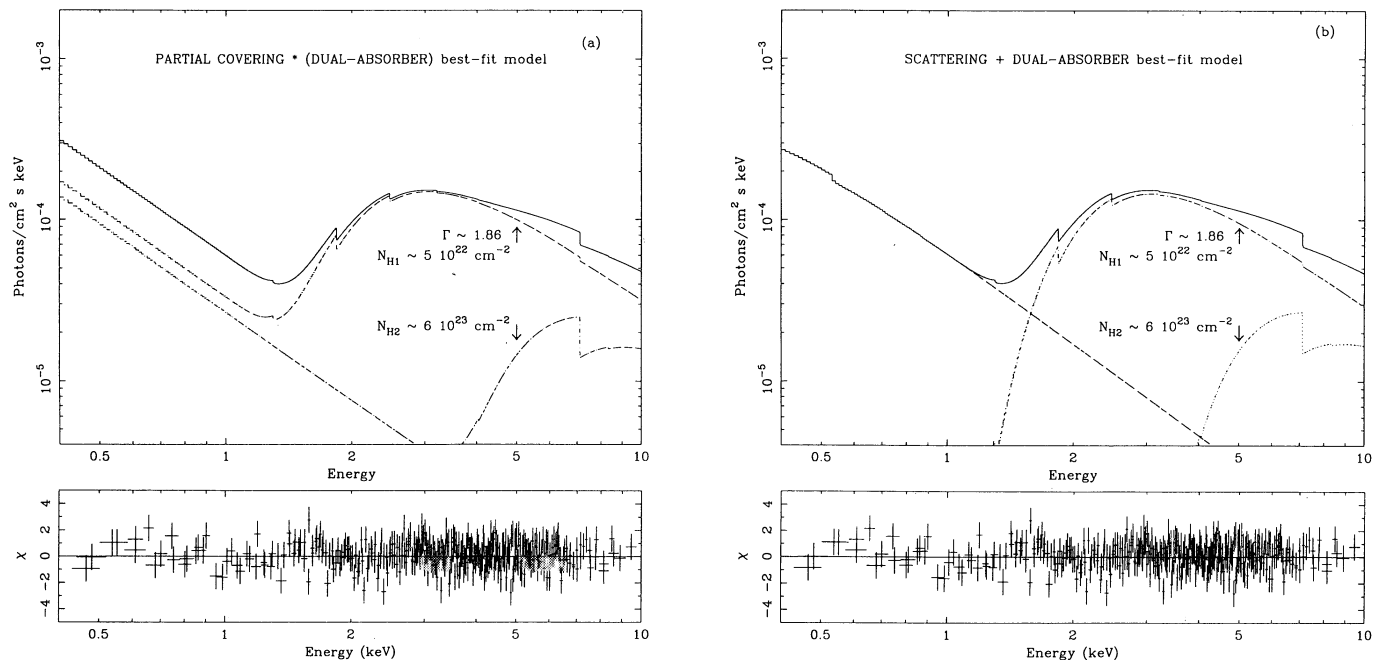
FIG. 6.—(a) SIS best-fit model and associated residuals with the partial covering + "dual-absorber" model. (b) SIS best-fit model and associated residuals with the scattering + "dual-absorber" model.

density, whereas part of the continuum emission is scattered into the line of sight by highly ionized matter present in the vicinity of the nucleus.

3.4. Iron Emission Line

We inspected the SIS spectra for the presence of an iron emission-line feature, and our results are summarized in Table 8.

With the continuum described by a thermal component plus an absorbed power law ($\Gamma \sim 1.2$), as given in § 3.2.1, we obtain an upper limit for the equivalent with of an iron $K\alpha$ line of EW $\lesssim 120$ eV. With the single partial covering model ($\Gamma \sim 1.45$, § 3.2.2), though the feature is only marginally visible in the data (Fig. 2), a narrow emission line is detected. The inclusion of a narrow line at the fixed energy $E = 6.254$ keV improves the fit to more than 99.5% confidence level ($\Delta\chi^2 \simeq 8$ for 311 dof). With the energy of the line free to vary, the best-fit value found is EW $\simeq 90^{+63}_{-49}$ eV when the width is fixed to 0, and EW $\simeq 100^{+62}_{-59}$ eV when the width is free, with $\sigma \lesssim 118$ eV (Table 8). These results agree with the emission of a fluorescent narrow Fe $K\alpha$ line from matter in a neutral state (Makishima 1986).

With the continuum modeled by a partial covering plus reflection component, the line becomes slightly weaker, with EW $\simeq 78^{+44}_{-53}$ eV. This value is of particular interest because it

TABLE 8
SIS: Fe K Line Best-Fit Parameters

Continuum Model	E (keV)	σ (eV)	EW (eV)
Raymond-Smith + power law......	$6.25^{+0.05}_{-0.16}$	0 (fixed)	$\lesssim 120$
Partial covering.....................	$6.25^{+0.05}_{-0.07}$	0 (fixed)	90^{+63}_{-49}
Partial covering.....................	$6.25^{+0.05}_{-0.03}$	$\lesssim 118$	100^{+62}_{-59}
Partial covering + reflection	$6.24^{+0.07}_{-0.08}$	0 (fixed)	78^{+44}_{-53}

NOTE.—Intervals are at 90% confidence for one interesting parameter.

can be directly compared with the expected EW from the reflection component, as shown in § 4.2.

The line is remarkably weak when compared to reported values for other Seyfert 2 galaxies (e.g., Kunieda et al. 1994). As far as results from the iron-line diagnostics are concerned, there is no need for "complex" geometries in the case of NGC 5252. A simple line-of-sight absorber, uniformly distributed around the source, can explain the observed iron line intensity of NGC 5252 (Makishima 1986; Leahy & Creighton 1993). We emphasize that no absorption edge, expected from neutral matter, has been detected at the redshifted energy of $E = 6.94$ keV. The upper limit derived is $\tau \lesssim 0.16$ at a 90% confidence level. At higher energies there is no evidence for a Fe K edge produced by ionized matter either.

4. DISCUSSION

4.1. Soft Excess

We have shown that the observed strong excess in NGC 5252 can well be described by either a scattering model or a partial covering model. Thermal models are unlikely.

Recent ASCA observations clearly detected thermal emission associated with starburst activity from the stereotype Seyfert 2 galaxy NGC 1068 (Ueno et al. 1994). A similar component is unlikely in the case of NGC 5252; its host galaxy is an early-type galaxy that does not exhibit strong stellar activity. More specifically, given a far-infrared luminosity of $\sim 6 \times 10^9 L_\odot$, the fitted soft X-ray luminosity of $L_X(0.4-2$ keV$) \sim 6 \times 10^{41}$ ergs cm^{-2} s^{-1} exceeds the value expected from the far-infrared/X-ray luminosity correlation for bright infrared normal and starbust galaxies (David, Jones, & Forman 1992) by approximately two orders of magnitude. This strongly suggests that the AGN inside NGC 5252 is directly responsible for the observed soft excess and excludes strong stellar activity (e.g., X-ray binaries and supernova remnants) associated with the host galaxy. Moreover, a hot thin collisionally ionized plasma at a temperature of

$T \sim 9 \times 10^6$ K should produce a blend of emission lines (mostly from Fe L) in the energy range 0.8 to 1.2 keV, which is not detected (§ 3.2.1). A one-temperature thermal plasma is therefore ruled out by the data, unless the metal abundances are very small ($\lesssim 0.01$ solar).

As long as the scattering zone is not highly ionized ($T \sim 10^5$ K), the scattering model predicts the presence of oxygen absorption edges between 530 and 870 eV, depending on the ionization state. An estimate of the expected oxygen depth τ_O due to the scattering material is given by $\tau_O \sim A_O f_{scatt} \sigma_O (\sigma_e c_f \times \Omega/4\pi)^{-1}$ (Weaver et al. 1994a), where A_O, f_{scatt}, σ_O, σ_e, c_f, and $\Omega/4\pi$ are the oxygen abundance, the fraction of scattered flux, the oxygen and electron scattering cross sections, the covering fraction, and the solid angle of the scattering matter, respectively. From the measured opening angle of approximately 75° for the ionization cones and the best-fit value $f_{scatt} \sim 0.04$, assuming $c_f = 1$ for the scattering medium and cosmic abundances, we estimate a value of $\tau_O \sim 11$. However, there is no evidence for such a strong edge in our data. As an example, the upper limit we measure for the O VIII edge at 0.85 keV (the strongest at soft energies) is $\tau \lesssim 1.5$. These results make the presence of a $T \sim 10^5$ K scattering matter in NGC 5252 unlikely.

If the scattering region is highly ionized, X-ray are efficiently scattered, and no absorption features are expected. Soft (~ 900 eV) emission lines, typically with EW $\lesssim 100$ eV, are instead expected for a highly photoionized gas (Netzer 1993). In the case of NGC 5252, the data do not allow significant detection of any soft X-ray feature but cannot rule out soft emission lines of up to several hundreds eV, either. The existence of a hot ($T \sim$ few $\times 10^6$ K) gas has been postulated by Marshall et al. (1993) to explain the higher ionization states indicated by multiple Fe K and Fe L emission lines observed in the BBXRT spectrum of NGC 1068. Also in the case of NGC 5252, gas inside its bi-cone might be highly photoionized since it directly sees the nuclear source and therefore could scatter the X-ray continuum into our line of sight, producing the observed soft excess. Polarization of the optical-UV continuum light should then be detected along the ionizing bi-cone. The recent blue (3200–6200 Å) spectropolarimetric observations conducted by Kay (1994) are, however, not very encouraging, as no clear polarization was detected ($P \simeq 11\% \pm 11\%$). As proposed by the author, imaging polarimetry or spectropolarimetry with the slit aligned along the axis of the cone could be more fruitful.

On the other hand, the partial covering model (Holt et al. 1980) does not predict any soft X-ray line emission, as the observed soft radiation escapes directly from the source. Since no X-ray variability was detected with *ASCA*, it is impossible to distinguish between a partial covering and scattering model with the present data. High spatial resolution X-ray observations with the HRI onboard *ROSAT* could easily resolve some extended emission (if present), and/or optical/UV polarimetric observations could help to discriminate between these two models.

4.2. The Flat Spectrum Problem

The flat spectrum *and* weak iron line differentiates NGC 5252 from the majority of known Seyfert 2 galaxies. X-ray spectra of most Seyfert 1 galaxies are found to be consistent with a steep intrinsic spectrum ($\Gamma_{2-18 keV} \sim 1.8$–2.1, when reflection is accounted for) and relatively strong (EW ~ 120–160 eV) fluorescent iron lines (e.g., Nandra & Pounds 1994). *Ginga* observations of Seyfert 2 galaxies (Awaki et al. 1991) and

recent *ASCA* observations (e.g., NGC 6552, Fukazawa et al. 1994; NGC 1068, Ueno et al. 1994) indicate that several Seyfert 2 galaxies have a flat hard X-ray spectrum and a strong (EW $\sim$ several hundred eV) fluorescence iron line (Kunieda et al. 1994).

These features (flat spectrum and strong iron line), first detected by *Ginga* and now confirmed by *ASCA*, are often interpreted as the signature of reflection of radiation from cold matter (e.g., Reynolds et al. 1994). In the case of NGC 5252, results from § 3.3.1 show that the data require a very strong ($R \sim 7$) reflection component to explain the observed flat spectrum. This high amount of reflection, if true, implies an anisotropic radiation field, i.e., the reflector "sees" more radiation than is observed directly (Ghisellini et al. 1991) and/or that there is a time lag effect. However, we believe that a substantial contribution from a reflection component is unlikely because it predicts a stronger iron line than observed. In fact, assuming cosmic abundances, the equivalent width (EW$_{refl}$) of the iron line relative to the reflection component (measured at the line energy) is of the order of approximately 1 keV. We obtained this result from performing Monte Carlo simulations in the simplest case of a slab geometry (Lightman & White 1988), but as a rough estimate it holds for almost all geometries and for a wide range of column densities (10^{22} to 10^{24} cm^{-2}) of the reflecting matter (see Makishima 1986; Awaki et al. 1991 for calculations with spherical and toroidal geometries, respectively). With the relationship EW$_{refl} \sim 1$ keV, the best-fit reflection model predicts an equivalent width (calculated with respect to the power-law plus reflection continuum) of $\simeq 400 \pm 250$ eV for the iron line. This value is about 5 times larger than the value (EW $\simeq 78 \pm 50$, § 3.4) measured from the data. One should point out that the two values are still consistent within 90% confidence (for two interesting parameters) because of the large errors associated with the parameters of the reflection component, but they exclude each other at the 1 σ level. The lack of a strong iron line in NGC 5252 suggests that a strong contribution from a reflection component, as a possible explanation of the flat spectrum, is unlikely.

One possible objection to the above comes from the edge-on geometry of NGC 5252, as inferred from optical observations discussed in § 1. Our previous assumption of a slab observed face-on (the inclination was fixed to 0 in § 3.3.1) may not be correct, and a larger inclination angle might have been more natural. However, the effect of a higher inclination would be to diminish the "efficiency" of the reflection. This effect would therefore be compensated in the fitting procedure by an increase of the normalization of the reflection component, leaving the above conclusions unchanged. It could also be argued that a different geometry for the reflector, like that of a (neutral) broad-line region (Yaqoob et al. 1993a; Nandra & George 1994) or a molecular torus (Ghisellini et al. 1994; Krolik, Madau, & Zycki 1994) may provide an alternative description for the observed spectral flatness. However, in all cases we would have to face the problem of the absence of a strong iron line.

Of course, if the Fe abundances are reduced, the value of the EW can be made to match the observed one. However, we do not regard this as a realistic possibility, as observational evidence indicates that, at least for some Seyfert 2 galaxies, the tendency is to have Fe overabundances. Another alternative possibility comes from theoretical arguments. Ross & Fabian (1993) and Zycki & Czerny (1994) showed that for a range of ionization stage of ions within $15 \lesssim <$Fe$> \lesssim 22$, or if iron is

fully ionized, the Fe line EW can be very low even in the presence of strong reflection. However, it should be emphasized that the presence of highly ionized material is compatible only with the case of reflection from an accretion disk or, possibly, from a broad-line region (Netzer 1993), but not from a torus. Moreover, in the case of ionized reflection, the substantial lack of photoelectric absorption yields a slope of the reflection component that is typically the same (or even steeper) than that of the intrinsic power law. The Fe K line center energy is also expected at slightly higher energies than observed if the gas is ionized. Therefore, the use of ionized reflection instead of neutral reflection would not be justified in this case.

We also found that a dual-absorber model (§ 3.3.3) could explain the observed flat spectrum with an intrinsically steep power law ($\Gamma \simeq 1.86 \pm 0.3$). The deduced spectral shape (Fig. 6a or 6b) is very similar to that expected with a reflection component (Fig. 4), but in this case a strong emission line is not expected a priori. The only constraint could come from the absorption edge at the redshifted energy of 6.94 keV, as expected by neutral absorption. The model predicts an absorption edge with optical depth $\tau \simeq 0.21^{+0.68}_{-0.11}$, which is consistent with the measured upper limit of $\tau \lesssim 0.16$ (see § 3.4). Therefore, nonuniform cold absorption provides an adequate explanation for the observed flat spectrum of NGC 5252. The absorbing material may be interpreted as a distribution of clouds with nonuniform density. Alternatively, it may consist of an absorbing torus with nonuniform density. In this case, since the absorption is approximately 10^{22-23} cm^{-2}, while predicted columns of absorption tori are approximately 10^{24-25} cm^{-2}, either (1) the torus is intrinsically optically thin, or (2) we are looking through its rim.

Another possible interpretation for the flat spectrum of NGC 5252 is that it is intrinsically flat. In a reanalysis of *Ginga* data, Smith & Done (1995) found several other Seyfert 2 galaxies with flat power-law spectra similar to that observed in NGC 5252, but with slightly higher iron-line EW $\sim$ 100–150 eV. These authors also found that at least four of the sources are incompatible with a steep slope, even with the inclusion of a reflection component. A recent analysis of combined *Ginga* and OSSE data by Zdziarski et al. (1994) indicate that the intrinsic X-ray spectra of some Seyfert 2 galaxies may be substantially harder than those of Seyfert 1 galaxies, in contrast to unified models of AGNs. Their slopes are consistent with our results for NGC 5252.

Finally, we would like to comment on the strong resemblance between the *ASCA* X-ray spectrum of NGC 5252 and the BBXRT and *ASCA* spectra of NGC 4151 (Weaver et al. 1994a, b). Both sources reveal a strong [$L_X(0.1-2.0) \sim 10^{41}$ ergs s^{-1}] soft excess below approximately 2 keV, an absorption around 10^{22-23} cm^{-2}, a flat continuum ($\Gamma \sim 1.3$–1.7), a high ($\gtrsim 0.90$) covering fraction, and a relatively weak iron line ($\sim$ 50–150 eV) (Yaqoob et al. 1993b; Weaver et al. 1994b). Both objects are relatively low luminosity Seyfert galaxies with $L_X(2-10$ keV$) \sim 2 \times 10^{43}$ ergs s^{-1} (NGC 5252) and $L_X(2-10$

keV) $\sim 10^{43}$ ergs s^{-1} (NGC 4151; Seyfert 1.5). These strong similarities suggest that the hard spectrum of NGC 5252 may be intrinsically flat, as seems to be the case for NGC 4151.

A better understanding of these Seyfert galaxies with flat spectra is of fundamental importance, not only because the problem has direct implications for unified models, but also because they could help explaining the so-called spectral paradox (Boldt 1987), i.e., the difference between the X-ray spectra of AGNs and that of the cosmic X-ray background (CXB).

5. CONCLUSION

The analysis of the X-ray spectrum of NGC 5252 shows that a single absorbed power law alone can describe the 0.7–10 keV GIS spectrum, but there is evidence of a strong soft excess in the 0.4–10 keV SIS spectrum. We argue against a thermal origin of the soft excess because there is no indication of starburst activity in NGC 5252, and we do not observe the expected soft emission lines produced by a plasma at $T \sim 10^6$ K.

The best description for the 0.4–10 keV spectrum is provided by a partial covering model or a scattering model, both models being equally compatible with the current data. The main results of the spectral analysis are a very flat ($\Gamma \simeq 1.45 \pm 0.23$) power law, a high covering fraction ($C_f \simeq 0.96 \pm 0.01$) from thick ($N_H \simeq 4.3 \pm 0.6 \times 10^{22}$ cm^{-2}) material, and a weak (EW $\simeq 90 \pm 60$ eV) iron line. The scattering model gives the same best-fit parameters, with a fraction about 4% of scattered light.

The flat spectral shape is incompatible with current theories of Seyfert unification schemes which predict steeper intrinsic power laws of $\Gamma \sim 1.8$–2.1. The flat slope *and* weak Fe K iron line measured in NGC 5252 make the reflection hypothesis unlikely, but it cannot be ruled out. The inclusion of a warm absorber, instead of a neutral absorber to explain the flat spectrum, gives systematic deviations at higher enegies, yielding a fit statistically worse than with only partial covering. A complex partial covering model with two different column densities (composite dual-absorber model) with a canonical steep ($\Gamma \sim 1.9$) power law offers a potential explanation for the flatness of the spectrum. An alternative interpretation of the present data is that the measured X-ray spectrum of NGC 5252 is intrinsically flat.

REFERENCES

Antonucci, R. R. J. 1993, ARA&A, 31, 473
Antonucci, R. R. J., & Miller, J. S. 1985, ApJ, 297, 621
Arnaud, K. A., et al. 1991, XSPEC User's Guide (ESA TM-09)
Avni, Y. 1976, ApJ, 210, 642
Awake, H., et al. 1991, PASJ, 43, 195
Boldt, E. 1987, Phys. Rep., 146, 215
David, L. P., Jones, C., & Forman, W. 1992, ApJ, 388, 82
Dickey, J. M., & Lockman, F. J. 1990, ARA&A, 28, 215
Fabian, A. C., et al. 1994, PASJ, 46, L59
Ferland, G. J. 1991, OSU Internal Rep., No. 91-01
Fukazawa, Y., et al. 1994, PASJ, 46, L141
Ghisellini, G., et al. 1991, MNRAS, 248, 14
Ghisellini, G., Haardt, F., & Matt, G. 1994, MNRAS, 267, 743
Guilbert, P. W., & Rees, M. J. 1988, MNRAS, 233, 475
Holt, S. S., et al. 1980, ApJ, 241, L13
Kay, L. 1994, ApJ, 430, 196

Kotilanien, J., & Prieto, M. A. 1994, A&A, 295, 649
Koyama, K., et al. 1989, PASJ, 41, 731
Krolik, J. H., & Kriss, G. A. 1995, preprint
Krolik, J. H., Madau, P., & Zycki, P. T. 1994, ApJ, 420, L57
Kunieda, H., et al. 1994, in New Horizon of X-ray Astronomy, ed. F. Makino
    & T. Ohashi (Tokyo: Universal Academy), 317
Lampton, M., Margon, B., & Bowyer, S. 1976, ApJ, 208, 177
Leahy, D. A., & Creighton, J. 1993, MNRAS, 263, 314
Lightman, A. P., & White, T. R. 1988, ApJ, 335, 57
Makishima, K. 1986, in Lecture Notes in Physics, Vol. 266, The Physics of
    Accretion onto Compact Objects, ed. K. O. Mason, M. G. Watson & N. E.
    White (Berlin: Springer), 249
Marshall, F. E., et al. 1993, ApJ, 405, 168
Matsuoka, M. 1994, in New Horizon of X-Ray Astronomy, ed. F. Makino &
    T. Ohashi (Tokyo: Universal Academy), 305
Miller, J. S., & Goodrich, R. W. 1990, ApJ, 355, 456
Morrison, R., & McCammon, D. 1983, ApJ, 270, 119
Nandra, K., & George, I. M. 1994, MNRAS, 267, 974
Nandra, K., & Pounds, K. A. 1994, MNRAS, 268, 405
Netzer, H. 1993, ApJ, 411, 594

Otani, C., & Dotani, T. 1994, ASCA News, 2, 25
Prieto, M. A., & Freudling, W. 1993, ApJ, 418, 668
———. 1995, MNRAS, submitted
Raymond, J. C., & Smith, B. W. 1977, ApJS, 35, 419
Reynolds, C. S., et al. 1994, MNRAS, 268, L55
Ross, R. R., & Fabian, A. C. 1993, MNRAS, 261, 74
Ruiz, M., Rieke, G., & Schmidt, G. 1994, ApJ, 423, 608
Smith, D. A., & Done, C. 1995, MNRAS, submitted
Tadhunter, C., & Tsvetanov, Z. 1989, Nature, 341, 422
Tran, H. D., Miller, J. S., & Kay, L. E. 1992, ApJ, 397, 452
Ueno, S., et al. 1994, PASJ, 46, L71
Unger, S. W., et al. 1987, MNRAS, 228, 671
Weaver, K. A., Arnaud, K. A., & Mushotzky, R. F. 1995, ApJ, 447, 121
Weaver, K. A., et al. 1994a, ApJ, 423, 621
———. 1994b, ApJ, 436, L27
Wilson, A. S., & Tsvetanov, Z. I. 1994, AJ, 107, 1227
Yaqoob, T., et al. 1993a, ApJ, 416, L5
———. 1993b, MNRAS, 262, L435
Zdziarski, A. A., et al. 1994, ApJ, 438, L63
Zycki, P. T., & Czerny, B. 1994, MNRAS, 266, 653